

**Convective damping  
of buoyancy  
anomalies**

I. Folkins

# Convective damping of buoyancy anomalies and its effect on lapse rates in the tropical lower troposphere

**I. Folkins**

Department of Physics and Atmospheric Science, Dalhousie University, Halifax, Nova Scotia, B3H 3J5, Canada

Received: 29 July 2005 – Accepted: 6 August 2005 – Published: 23 August 2005

Correspondence to: I. Folkins (ian.folkins@dal.ca)

© 2005 Author(s). This work is licensed under a Creative Commons License.

Title Page

Abstract

Introduction

Conclusions

References

Tables

Figures

⏪

⏩

◀

▶

Back

Close

Full Screen / Esc

Print Version

Interactive Discussion

EGU

## Abstract

In actively convecting regions of the tropics, lapse rates in the lower troposphere (2.0 km to 5.2 km) vary with height in a way which is inconsistent with both reversible moist adiabatic and pseudoadiabatic assumptions. It is argued that this anomalous behavior arises from the tendency for the divergence of a convective buoyancy anomaly to be primarily offset by the collective divergence of all other updrafts and downdrafts within one Rossby radius of deformation. (Ordinarily, convective divergences are at least partially offset by an induced radiative divergence in the background atmosphere.) If convective divergences are balanced purely by other convective divergences, it would force the vertical clear sky radiative mass flux to be independent of altitude. This is consistent with what is observed at several radiosonde locations in the Western Tropical Pacific between 2.0 and 5.2 km. It is conjectured, that at tropical locations where SST's exceed 27°C over a region whose horizontal extent exceeds the local Rossby radius, this condition on the clear sky radiative mass flux serves to partially constrain the range of physically allowed mean temperature and moisture profiles in the lower troposphere.

### 1. Introduction

It is commonly accepted that the mean temperature profile in the tropics approximately follows a moist adiabat. If one starts at the surface with an air parcel with typical values of temperature and relative humidity, and lifts this air parcel upward along a moist adiabatic trajectory, one generates a temperature profile that is close to the tropical mean. It is not obvious why the tropical atmosphere should have this property. Unlike the establishment of dry adiabatic layers in well mixed layers, this process cannot depend on direct physical mixing, since deep convective updrafts cover only a small fraction of the tropics. The process is instead believed to be mediated by gravity waves. Gravity waves propagate outward from buoyancy anomalies such as those associated with

## Convective damping of buoyancy anomalies

I. Folkins

Title Page

Abstract

Introduction

Conclusions

References

Tables

Figures

◀

▶

◀

▶

Back

Close

Full Screen / Esc

Print Version

Interactive Discussion

---

**Convective damping  
of buoyancy  
anomalies**I. Folkins

---

[Title Page](#)[Abstract](#)[Introduction](#)[Conclusions](#)[References](#)[Tables](#)[Figures](#)[◀](#)[▶](#)[◀](#)[▶](#)[Back](#)[Close](#)[Full Screen / Esc](#)[Print Version](#)[Interactive Discussion](#)

EGU

deep convection, and give rise to vertical motions in the background atmosphere that modify the density profile of the background atmosphere in such a way as to diminish the buoyancy of the heat source (Bretherton and Smolarkiewicz, 1989). For example, positively buoyant warm anomalies heat the atmosphere by induced descent, while negatively buoyant cold anomalies cool the atmosphere by induced ascent. A heat source in which the temperature profile followed a moist adiabat would be expected to drive the background atmosphere toward a stratification which was also approximately moist adiabatic.

There are several difficulties with accepting this explanation of the temperature structure of the tropical troposphere. One difficulty is that lapse rates in the lower troposphere of actively convecting regions deviate significantly from those predicted by moist adiabatic ascent (Mapes, 2001; Folkins and Martin, 2005). In addition, many observations have shown that updrafts speeds are much smaller than predicted by undilute parcel ascent, and, although updrafts are on average slightly positively buoyant, they exhibit a wide range of both positive and negative buoyancies (Jorgensen and LeMone, 1989; Lucas et al., 1994; Wei et al., 1998). These observations presumably reflect the efficiency of entrainment in the lower tropical troposphere, and are inconsistent with the view updrafts in the lower troposphere are undilute, and as such, would be in a position to impose a moist adiabatic density profile on the background atmosphere. Finally, the density of the lower troposphere is likely to be affected by gravity waves from both updrafts and downdrafts. In the lower troposphere, the downdraft mass flux is comparable to the updraft mass flux (May and Rajopadhyaya, 1999). The majority of these downdrafts are probably unsaturated, since those originating from the mid-troposphere would be starting out with low values of equivalent potential temperature, and if saturated, would generate much larger negative buoyancies than observed (e.g. Wei et al., 1998). The gravity waves generated by these unsaturated downdrafts would not be expected to drive the atmosphere toward a moist adiabatic temperature profile. The impact of downdrafts on mean tropical temperatures is usually not considered. It would, however, be desirable to have some explanation for the observed

## Convective damping of buoyancy anomalies

I. Folkins

Title Page

Abstract

Introduction

Conclusions

References

Tables

Figures

◀

▶

◀

▶

Back

Close

Full Screen / Esc

Print Version

Interactive Discussion

EGU

density structure of the lower tropical troposphere which treated the effects of updrafts and downdrafts on the density of the background atmosphere in a more symmetric manner.

In this paper, the observed temperature structure of the tropical lower troposphere is attributed to the tendency of updrafts and downdrafts to produce zero net mass divergence, averaged over an appropriate spatial scale. It will be shown that this is the type of constraint that would be expected in the limit that entrainment and detrainment are extremely efficient at damping buoyancy anomalies. The argument relies on a conceptual separation of the atmosphere into convective and background domains.

The convective domain is defined as that portion of the atmosphere whose density is significantly different from the regional mean, does not obey hydrostatic balance, and is therefore a source of gravity waves to the background atmosphere. Anomalous buoyancies within the convective domain give rise to vertical velocities that help drive turbulent exchange with the background atmosphere. Density variations in the tropics usually originate from condensational heating or evaporative cooling, and are therefore associated with cloud droplets and/or precipitation. The diabatic heating inside the convective portion of the domain will also be modified by cloud radiative heating, and eddy heat fluxes divergences associated with turbulent motions. In the background domain, it is assumed that clear sky radiative heating is the only source of diabatic heating. Let  $\overline{\omega}_c$  and  $\overline{\omega}_b$  refer to the vertical velocities of the convective and background domains, horizontally and temporally averaged over some convectively active region. If  $\overline{\omega}_t$  refers to the total vertical velocity of the region, then

$$\overline{\omega}_t = \overline{\omega}_c + \overline{\omega}_b. \quad (1)$$

Since the divergence is just the vertical gradient of the vertical velocity (i.e.  $\delta_t = -\frac{\partial \omega_t}{\partial p}$ , etc.), this implies

$$\overline{\delta}_t = \overline{\delta}_c + \overline{\delta}_b. \quad (2)$$

From this equation, we arrive at a constraint on temperatures in the lower troposphere by (i) using ECMWF horizontal winds to show that  $\overline{\delta}_t \sim 0$  when averaged over spatial

---

**Convective damping  
of buoyancy  
anomalies**I. Folkins

---

[Title Page](#)[Abstract](#)[Introduction](#)[Conclusions](#)[References](#)[Tables](#)[Figures](#)[◀](#)[▶](#)[◀](#)[▶](#)[Back](#)[Close](#)[Full Screen / Esc](#)[Print Version](#)[Interactive Discussion](#)

EGU

scales larger than 2000 km in the tropical lower troposphere, and (ii) arguing that updrafts and downdrafts in the lower troposphere should conspire to make the convective divergence  $\overline{\delta_c} \sim 0$  over a similar spatial scale. Constraints (i) and (ii), if true, would also imply that  $\overline{\delta_b} \sim 0$  on spatial scales larger than 2000 km, and force the background vertical radiative mass flux  $\overline{\omega_b}$  to be independent of altitude in the lower troposphere, a result that is consistent with observations. In this view, a divergence constraint on the convective mass flux gives rise to a background clear sky radiative mass flux in which is independent of altitude. Since there are a variety of joint temperature and relative humidity profiles that would give rise to a clear sky radiative mass flux that was independent of altitude, this would serve as a coupled constraint on the covariation of humidity and temperature profiles in the tropical lower troposphere. Temperature and moisture profiles in the tropics are, of course, also constrained by the range of physically allowed rates of entrainment and detrainment that would make densities within updrafts and downdrafts similar to those of the background atmosphere.

In the next section, the arguments of the previous paragraph are motivated by a discussion of observed lapse rates in an actively convecting region. The arguments are then restated in Sects. 3–5. Much of the rest of the paper revolves around a discussion of why one might anticipate the emergence of an entrainment-dominated (or buoyancy-repressed) regime in the lower troposphere (2 km–5.2 km), but not in the mid-troposphere (5.2 km–10 km).

## 2. Lapse rate profiles in actively convecting regions

During convective adjustment, gravity waves propagating outward from buoyancy anomalies give rise to net vertical displacements in the background atmosphere which drive the density profile of the atmosphere toward the mean updraft/downdraft density. In addition to temperature and pressure, the density of an air parcel depends on the humidity and condensate loading of the air parcel. In the background atmosphere, or during pseudoadiabatic ascent (where all condensate is assumed to be immediately

## Convective damping of buoyancy anomalies

I. Folkins

Title Page

Abstract

Introduction

Conclusions

References

Tables

Figures

◀

▶

◀

▶

Back

Close

Full Screen / Esc

Print Version

Interactive Discussion

EGU

removed), the appropriate density variable is virtual temperature  $T_v$ . During reversible moist adiabatic ascent (where it is assumed that all condensate is retained by the air parcel), the appropriate density variable is the density temperature  $T_\rho$ . The dashed line in Fig. 1 shows the  $dT_v/dz$  of a moist pseudoadiabat with a pseudoequivalent potential temperature ( $\theta_{ep}$ ) (Bolton, 1980) equal to 350 K. This value of  $\theta_{ep}$  generates a lapse rate which is in good agreement with the observed lapse rate between 5.2 km and 10 km. The dotted line in Fig. 1 shows the  $dT_\rho/dz$  of reversible moist adiabat with  $\theta_e=350$  K. (The reversible density temperature was not calculated above the melting level because doing so would require an assumption about the phase of the condensate. In any event, the assumption that all condensate is retained by the air parcel can be expected to become increasingly unrealistic in the upper troposphere.) Below the melting level, the reversible adiabat is in better agreement with the observed lapse rate than the pseudoadiabat (see also Betts, 1982; Xu and Emanuel, 1989). However, neither the reversible or pseudoadiabatic idealizations are able to reproduce the shape of the observed notch in  $dT_v/dz$  between 2 km and 5.2 km (Folkins and Martin, 2005).

Convective adjustment involves an interaction between a buoyancy anomaly and the background atmosphere. One can think of an updraft or downdraft as trying to force the background atmosphere to adopt some preferred density profile (e.g. moist adiabatic). This perspective is somewhat one-sided, however, because this process usually also involves the turbulent exchange of air between a buoyancy anomaly and the background atmosphere, and in the process of this exchange, the density of the buoyancy anomaly can be significantly altered. Updrafts typically entrain air from their environment at altitudes where their buoyancy is increasing, and detrain air into their environment at altitudes where their buoyancy is diminishing (Bretherton and Smolarkiewicz, 1989). The height ranges of preferred entrainment or detrainment can be identified from profiles of  $\theta_{ep}$  and saturated pseudoequivalent potential temperature ( $\theta_{ep}^*$ ). Figure 2 shows annual mean profiles of  $\theta_{ep}$  and  $\theta_{ep}^*$  above Koror. The buoyancy of an air parcel is proportional to the difference between its  $\theta_{ep}$  and the  $\theta_{ep}^*$  of the background atmosphere (assuming that the effects of water vapor and condensate loading

---

**Convective damping  
of buoyancy  
anomalies**I. Folkins

---

[Title Page](#)[Abstract](#)[Introduction](#)[Conclusions](#)[References](#)[Tables](#)[Figures](#)[◀](#)[▶](#)[◀](#)[▶](#)[Back](#)[Close](#)[Full Screen / Esc](#)[Print Version](#)[Interactive Discussion](#)

EGU

on density are small). The  $\theta_{ep}$  of an air parcel is approximately conserved during saturated and unsaturated vertical displacements. As shown in Fig. 2, an air parcel lifted upward from the surface with  $\theta_{ep}=356$  K is initially negatively buoyant. However, once it crosses its Level of Free Convection (LFC) near 0.7 km, its  $\theta_{ep}$  diverges from the background  $\theta_{ep}^*$ , and it will become progressively more positively buoyant. In the lower troposphere, updrafts can therefore be expected to entrain air from their environment. Above the melting level, where the atmosphere is stable and  $\theta_{ep}^*$  increases gradually with height, updrafts would be expected to slowly detrain air into the background atmosphere as they become less buoyant.

By the same reasoning, downdrafts are expected to detrain air into the background atmosphere above the melting level, while entraining air from the background atmosphere below the melting level. Figure 2 shows that a downdraft originating at 8 km will lose negative buoyancy as it approaches the  $\theta_{ep}^*$  curve, while a downdraft originating near 4 km will gain negative buoyancy as it diverges from the  $\theta_{ep}^*$  curve.

It was mentioned earlier that, in the standard view, one thinks of convective adjustment as driving the atmosphere toward some preferred density profile. This is somewhat of a simplification, however, because convective plumes which maintained a fixed buoyancy offset from the background atmosphere could, in principle, have zero net mass exchange with the background atmosphere. In this case, one would think of the convective plumes as imposing a vertical density gradient (or virtual temperature lapse rate) on the background atmosphere, rather than a specific density profile. For example, Fig. 1 shows that the  $\theta_{ep}$  which best describes the lapse rate between 5.2 km and 10 km is 350 K, a value which presumably reflects the mass weighted  $\theta_{ep}$  of updrafts in this interval. However, Fig. 2 shows that the mean  $\theta_{ep}^*$  of the background atmosphere increases from roughly 344 K to 346 K in this height range. There is therefore a 4–6 K offset between the  $\theta_{ep}$  of the pseudoadiabat from the surface which best approximates temperatures between 5.2 km and 10 km and the  $\theta_{ep}$  which best approximates the lapse rate. The magnitude of this offset may reflect the mean positive buoyancies of updrafts in this region of the troposphere.

### 3. The total divergence

This paper will attribute the anomalous behavior of the tropical lapse rate below the melting level (as shown in Fig. 1) to a divergence constraint on the vertical radiative mass flux of the background atmosphere. In the tropics, the spatial scale of divergence patterns is larger in the upper troposphere than in the lower troposphere. Figure 3 shows the rate at which areally averaged divergence decreases when, starting from an initial grid cell in which the divergence is positive, one averages progressively outward over larger and larger squares centered on the original grid cell. Figure 3 shows the average divergence of boxes of  $3\times 3$ ,  $5\times 5$ ,  $7\times 7$ ,  $9\times 9$ , and  $11\times 11$  grid cells. Only starting grid cells between  $10^\circ$  S and  $10^\circ$  N were considered. Divergence values were taken from the ERA-40 monthly mean ECMWF reanalysis for April 2000 (other months are similar). The ERA-40 reanalysis has a  $2.5^\circ$  zonal resolution, and a  $2.25^\circ$  meridional resolution. Between 300 mb and 100 mb, the spatial scale over which a positive divergence anomaly declines by  $1/e$  is typically 3000 km. Below 500 mb, this distance is typically 900 km. That is, a  $3\times 3$  box of grid cells, centered on a grid cell with positive divergence, typically has  $1/e$  of the areally averaged divergence of the center grid cell. Though not shown in Fig. 3, the distance over which a divergence anomaly declines by  $1/e$ , when starting out with a negative value of divergence, is also roughly equal to 900 km.

The gravity waves propagating outward from a convective source give rise to net vertical displacements which perturb the temperature of the background atmosphere. The horizontal distance to which these temperature perturbations extend is referred to as the Rossby radius of deformation. One would expect the spatial scale of a divergence pattern to be approximately equal to the Rossby radius of the gravity waves which have the most influence on background temperatures. The Rossby radius of a gravity wave is approximately given by  $\lambda_r = c/f$ , where  $c$  is the gravity wave speed and  $f$  is the Coriolis parameter. Convective sources generate gravity waves with a variety of speeds, so that such sources cannot be characterized by a single Rossby radius.

## Convective damping of buoyancy anomalies

I. Folkins

Title Page

Abstract

Introduction

Conclusions

References

Tables

Figures

◀

▶

◀

▶

Back

Close

Full Screen / Esc

Print Version

Interactive Discussion

## Convective damping of buoyancy anomalies

I. Folkins

Title Page

Abstract

Introduction

Conclusions

References

Tables

Figures

◀

▶

◀

▶

Back

Close

Full Screen / Esc

Print Version

Interactive Discussion

EGU

It has been suggested, however, that deep convective sources preferentially generate gravity waves with speeds of  $c \sim 24$  m/s and  $c \sim 50$  m/s (Mapes and Houze, 1995). At a latitude of  $10^\circ$ , these wave speeds corresponds to Rossby deformation radii of 960 km and 2000 km. The proximity of 960 km to the lower tropospheric e-folding distance of 900 km is consistent with the view that the spatial variability of the divergence field in the lower troposphere is dominated by the slower, higher wavelength stratiform mode.

In the Western tropical Pacific, climatological rainfall patterns from the NCEP, NASA, and ECMWF reanalyses differ significantly from the observed rainfall pattern, and their upper tropospheric divergence patterns differ significantly from each other (Newman et al., 2000). It is likely that the variability of tropical convection in most forecast models is weakly constrained by observations, and highly dependent on the model physics (especially on their convective schemes). In principle, it would be desirable to determine the spatial and temporal scale over which areally averaged lower tropospheric total divergence goes to zero from observations. This would require a sufficiently dense array of rawinsonde data, centered on an actively convecting region of the ocean, and of sufficiently large horizontal extent that it exceeded the local Rossby radius.

#### 4. The convective divergence

In the previous section, it was shown that the total divergence  $\overline{\delta_t}$ , as inferred from ERA-40 horizontal winds, was essentially equal to zero when areally averaged over spatial scales larger than 2000 km. In actively convecting regions of the tropics, most of the total divergence originates from vertical motions associated with convective heating and cooling. In this section, we show that there is a natural tendency for the divergences of updrafts and downdrafts to offset one another.

In a hypothetical atmosphere where the the buoyancy of every updraft/downdraft was constant, there would be no requirement for a net exchange of mass between updrafts/downdrafts and the background atmosphere. Suppose, however, that one introduced into this atmosphere a buoyancy anomaly in which the buoyancy increased

---

**Convective damping  
of buoyancy  
anomalies**I. Folkins

---

[Title Page](#)[Abstract](#)[Introduction](#)[Conclusions](#)[References](#)[Tables](#)[Figures](#)[◀](#)[▶](#)[◀](#)[▶](#)[Back](#)[Close](#)[Full Screen / Esc](#)[Print Version](#)[Interactive Discussion](#)

EGU

with height from negative to positive. The horizontal and vertical redistribution of mass in the background atmosphere associated with such an anomaly is shown in Fig. 5 (Bretherton and Smolarkiewicz, 1989). There would be a downward vertical velocity in the background atmosphere at heights where the buoyancy of the anomaly was positive, and an upward vertical velocity in the background atmosphere at heights where the buoyancy of the anomaly was negative. These induced vertical velocities would be associated with a convergent influx of air toward the anomaly, maximizing at the height where the buoyancy of the anomaly changed from negative to positive.

The vertical motions associated with a buoyancy anomaly give rise to temperature changes in the background atmosphere. These temperature changes would suppress both the convergent influx of air toward the buoyancy anomaly, and also generate a compensating divergent outflow of air from the surrounding updrafts and downdrafts. For example, the downward vertical velocity in the background atmosphere above the convergent inflow would warm the atmosphere. Conversely, the upward vertical velocity below the convergent inflow would cool the atmosphere. Both of these changes would reduce the magnitude of the buoyancy within the buoyancy anomaly. This would also reduce the buoyancy gradient inside the buoyancy anomaly, and reduce its induced convergent inflow.

The temperature changes of the background atmosphere also affect the buoyancies of surrounding updrafts and downdrafts. The negative buoyancy of the upper half of the downdraft would be increased, while the negative buoyancy of the lower half of the downdraft would be decreased. A downdraft whose negative buoyancy decreased toward the surface would tend to detrain air, and be associated with a divergent outflow. Similarly, temperatures changes in the background atmosphere would also give rise to buoyancy changes in surrounding updrafts which would contribute toward a divergent outflow of air.

Heat sources produce buoyancy and divergence anomalies which are collectively damped by surrounding updrafts and downdrafts. This damping arises from the inability of a finite region of a stratified, rotating atmosphere to accommodate arbitrary imposed

---

**Convective damping  
of buoyancy  
anomalies**I. Folkins

---

[Title Page](#)[Abstract](#)[Introduction](#)[Conclusions](#)[References](#)[Tables](#)[Figures](#)[⏪](#)[⏩](#)[◀](#)[▶](#)[Back](#)[Close](#)[Full Screen / Esc](#)[Print Version](#)[Interactive Discussion](#)

EGU

changes in its vertical mass distribution (e.g. Mapes and Houze, 1995). The response shown in Fig. 5 could be characterized as the dry response, since it does not directly consider the effects of cloud microphysics on buoyancy. These effects can, however, be quite significant. In the case of dry convection, the entrainment of colder environmental air into the updraft would diminish the buoyancy (warm bias) of the updraft, but leaves its buoyancy flux (product of the mass flux and the buoyancy) unchanged (Emanuel and Bister, 1996). In the case of moist convection, however, the effect of entrainment on the buoyancy of an updraft is a strong function of the condensate loading of the updraft, the relative humidity of the entrained air, and the temperature. The evaporation of liquid water or ice within the updraft, due to dry air entrainment, can rapidly cool the updraft, and in some cases, change its buoyancy from positive to negative. Buoyancy reversal is more likely in cases of high condensate loading and lower background relative humidity. In general, it is also more likely at warmer temperatures, where for a given background relative humidity and entrainment rate, more evaporation of condensate can occur. This self damping of a moist updraft due to the entrainment of unsaturated air represents an additional negative feedback on the strength of a convergence anomaly.

The effect of entrainment on the buoyancy of a downdraft is more complicated than that of an updraft. In general, it would be expected to reduce the negative buoyancy of a downdraft, since in the lower troposphere, one would usually be introducing air with a higher  $\theta_e$ . But the introduction of unsaturated air into a nearly saturated downdraft could also increase evaporative cooling, and thereby increase the negative buoyancy of the downdraft. The overall effect of entrainment on the negative buoyancy of a downdraft is probably determined by whether the entrained mixture has a higher or lower relative humidity than the unmixed air parcel. In areas of the tropical ocean where there is frequent deep convection and background relative humidities are quite high, entrainment probably decreases downdraft buoyancies.

## 5. The background divergence

In most of the troposphere, buoyancy forced divergence anomalies are partly balanced by changes in the convective divergence, and partly by changes in the radiative divergence of the background atmosphere. The vertical radiative mass flux can be expressed in terms of the radiative heating rate  $Q_r$  and static stability  $\sigma$

$$\omega_r = \frac{Q_r}{\sigma}. \quad (3)$$

The static stability is closely related to the lapse rate, and has various equivalent forms, including (e.g. Holton, 1992)

$$\sigma = \frac{(\Gamma_d - \Gamma)}{\rho g} = -\frac{T}{\theta} \frac{\partial \theta}{\partial p} = \frac{\partial}{\partial p} \left( \frac{h_d}{c_p} \right), \quad (4)$$

where  $\Gamma$  is the lapse rate ( $=-dT/dz$ ),  $\Gamma_d$  is the dry adiabatic lapse rate, and  $h_d = c_p T + gz$  is the dry static energy. In Fig. 4, the downward motion of the background atmosphere warms the background atmosphere, increases the radiative cooling rate, and favors an increased downward radiative mass flux. Conversely, the upward vertical motion in the lower part of the buoyancy anomaly cools the background atmosphere, decreases the radiative cooling rate, and favors a decreased downward radiative mass flux. The increased downward radiative mass above the convergence anomaly, and the decreased downward radiative mass flux below the convergence anomaly would imply a compensating divergent outflow from the background atmosphere toward the convergence anomaly.

Climatological profiles of the radiative cooling rate and static stability in actively convecting regions suggest that radiative damping of buoyancy anomalies in the lower troposphere is weak. Figure 4 shows the annual mean profile of static stability at Truk. The dashed line indicates the static stability profile generated by undilute pseudoadiabatic ascent from the surface, starting with an air parcel with pseudoequivalent potential temperature  $\theta_{ep}$  equal to 350 K. As would be anticipated from Fig. 1, it closely

### Convective damping of buoyancy anomalies

I. Folkins

Title Page

Abstract

Introduction

Conclusions

References

Tables

Figures

◀

▶

◀

▶

Back

Close

Full Screen / Esc

Print Version

Interactive Discussion

---

**Convective damping  
of buoyancy  
anomalies**I. Folkins

---

[Title Page](#)[Abstract](#)[Introduction](#)[Conclusions](#)[References](#)[Tables](#)[Figures](#)[◀](#)[▶](#)[◀](#)[▶](#)[Back](#)[Close](#)[Full Screen / Esc](#)[Print Version](#)[Interactive Discussion](#)

EGU

matches the observed static stability above the melting level, but fails to reproduce the notch in the observed  $\sigma$  between 2 km and 5.2 km. The blue curve in Fig. 5 is the rate of clear sky radiative cooling at Truk. It was obtained by averaging over the four seasonal mean  $Q_r$  profiles at Truk, each calculated from seasonal mean temperature, pressure, and relative humidity profiles. The heating rates calculated by the radiative transfer model (Fu and Liou, 1992) exhibit excellent agreement with line by line calculations (Gettelman et al., 2004). Roughly 500 radiosonde profiles were used to construct each seasonal mean. Below the melting level, the variation of the static stability with height is similar to the variation of the radiative cooling rate with height. This gives rise to a radiative mass flux which is roughly constant between 2 km and 5.2 km. The climatological clear radiative divergence at these locations is therefore small ( $\delta_r \sim 0$ ). It would also imply that the areally averaged divergence of the background atmosphere is small ( $\overline{\delta_b} \sim 0$ ), provided the  $\omega_r$  profiles shown in Fig. 5 are representative of other actively convecting locations, and the only source of diabatic heating in the background atmosphere is clear sky radiative heating.

In principle, the presence of clouds could significantly perturb lower tropospheric radiative heating rates from their clear sky values. It is likely, however, that effects of cloud radiative heating are concentrated within the clouds themselves. As such, cloud radiative heating would affect cloud buoyancies, but have a reduced impact on the diabatic heating of the background atmosphere. It can be shown, for example, that the vertical gradients of the clear sky heating rates shown in Fig. 5 are only weakly sensitive to the addition of an overhead cirrus anvil. It has also been noted that the clear sky component of radiative heating rates are essentially insensitive to different cloud distribution assumptions (Bergman and Hendon, 1998).

## 6. Origin of lower tropospheric minimum in radiative cooling

Radiative heating rates in the lower tropical troposphere are quite sensitive to specific humidity, but also to temperature, so that the vertical variation of  $Q_r$  depends, in part,

---

**Convective damping  
of buoyancy  
anomalies**I. Folkins

---

[Title Page](#)[Abstract](#)[Introduction](#)[Conclusions](#)[References](#)[Tables](#)[Figures](#)[◀](#)[▶](#)[◀](#)[▶](#)[Back](#)[Close](#)[Full Screen / Esc](#)[Print Version](#)[Interactive Discussion](#)

EGU

on the vertical variation of  $\sigma$ . This leads to some ambiguity in how to interpret a radiative mass flux  $\omega_r$  that is independent of altitude. If, for example, the lower tropospheric radiative cooling minimum shown in Fig. 4 is simply a linear response to the static stability minimum, then one would expect  $Q_r/\sigma$  to be independent of height, and the constancy of  $\omega_r$  between 2 km and 5.2 km would be an anticipated response to a particular temperature profile. On the other hand, if  $Q_r$  and  $\sigma$  were essentially independent of each other, it seems less likely that they would covary in such a similar way, and it would seem more plausible that temperature and specific humidity were mutually adjusting to satisfy an independent constraint on the radiative mass flux. In this section, it is shown that the radiative cooling minimum in the lower tropical troposphere is largely decoupled from the minimum in static stability.

To test whether the lower tropospheric minimum in radiative cooling was forced by the static stability minimum, we constructed a test temperature profile which was as close as possible to a real tropical temperature profile (the mean September–November profile at Koror), but in which the notch in static stability was removed. The dashed line in Fig. 6 shows the difference  $T_t - T_{\text{KOROR}}$  between the test and mean Koror temperature profiles. Below 1.8 km, and above 7.2 km, the test temperature profile was set equal to the Koror profile. Between 1.8 km and 7.2 km, the lapse rate of the test profile was forced to vary linearly with height. The temperature difference between the two profiles is everywhere less than 0.4 K. The radiative cooling rate of the “smoother” test profile is compared with that of the original Koror profile in Fig. 7. The differences are quite small, with the lower tropospheric cooling minimum slightly deeper for the test case. This demonstrates that the minimum in the cooling rate does not originate from the minimum in the static stability.

The test described in the previous paragraph confirms expectations from previous work that the radiative cooling minimum in the lower tropical troposphere is largely due to the low transmissivity to space of water vapor in this region of the atmosphere. Longwave radiative cooling rates in the lower troposphere are well reproduced by the “cooling to space” approximation (Rodgers and Walshaw, 1966), which can be written

(Mapes and Zuidema, 1996)

$$Q_r(z) = B(z)\sigma(z)T(z, \infty),$$

where  $B(z)$  is the Planck function,  $\sigma(z)$  is the extinction cross-section (proportional to the humidity), and  $T(z, \infty)$  is the transmission between height  $z$  and space. The higher temperatures and increased humidities of the lower tropical troposphere would tend to increase radiative cooling rates. However, this is more than offset by a rapid decrease in the transmissivity to space below 8 km (due to the increase in the overhead column of water vapor), leading to a reduction of cooling rates in the lower troposphere (Doherty and Newell, 1984).

## 7. Timescales of radiative and convective damping

It has been argued that, in the lower tropical troposphere, the rapid convective damping of buoyancy anomalies, and the requirement that the total divergence go to zero on spatial scales comparable with the Rossby radius of deformation, force the mean clear sky radiative mass flux to be independent of altitude. That is, temperatures and humidities in the lower troposphere are forced to mutually adjust to satisfy a constraint on the radiative mass flux. The degree to which buoyancy anomalies (and their associated divergences) are damped by convective versus radiative processes will depend on the respective timescales of each process. The observed weakness of buoyancy anomalies in the lower tropical troposphere (Jorgensen and LeMone, 1989; Lucas et al., 1994; Wei et al., 1998) is consistent with the view that the timescale for the total damping by both processes is very short. However, no argument has yet been advanced here as to why the timescale for a buoyancy anomaly to be convectively damped should be so much faster than the timescale for such an anomaly to be radiatively damped. There has also been no discussion as to why a transition between the convectively and radiatively damped regimes should occur near the melting level. Although definitive answers

## Convective damping of buoyancy anomalies

I. Folkins

Title Page

Abstract

Introduction

Conclusions

References

Tables

Figures

◀

▶

◀

▶

Back

Close

Full Screen / Esc

Print Version

Interactive Discussion

to these questions are beyond the scope of this paper, one can identify some factors which might contribute to their resolution.

The convective damping timescale should depend on the timescale on which the mass fluxes inside updrafts and downdrafts respond to temperature fluctuations in the background atmosphere. The melting level occurs near the minimum in  $\theta_{ep}^*$ , which denotes a transition from a conditionally unstable to stable atmosphere. In a conditionally unstable atmosphere, a saturated air parcel will immediately become positively buoyant when subjected to an upward positive velocity. It has positive Convective Available Potential Energy (CAPE) and zero Convective Inhibition (CIN). Although subsaturated air parcels in a conditionally unstable atmosphere will have a non-zero convective inhibition, temperature fluctuations can still trigger positive buoyancies in air parcels if the relative humidity of the air parcel is sufficiently high. Near the equator, where the Rossby radius is quite large, temperature perturbations from a buoyancy anomaly extend over a broad area. The likelihood that such a perturbation will trigger an updraft is therefore quite high, although clearly, it would be very sensitive to the background relative humidity.

The situation above the melting level is quite different. In general, it is not possible for an air parcel in an atmosphere where  $\theta_{ep}^*$  increases monotonically with height to have positive CAPE. There is an intrinsic upper limit on the upward cloud mass flux, set by the number of pre-existing air parcels at that height that are already positively buoyant.

One would also expect the downdraft mass flux to be more responsive to temperature fluctuations in a conditionally unstable atmosphere. Figure 2 shows that the  $\theta_{ep}$  trajectory of an undilute downdraft below the melting level diverges from the  $\theta_{ep}^*$  curve. From a thermodynamic perspective, every air parcel below the  $\theta_{ep}^*$  minimum is capable of descending to the surface given sufficient exposure to precipitation. Because the relative humidity of an undilute downdraft decreases as it descends, its ability to evaporate condensate is maintained. In contrast, the  $\theta_e$  trajectory of an undilute downdraft above the melting level tends to approach the  $\theta_{ep}^*$  curve. At this point, it

---

## Convective damping of buoyancy anomalies

I. Folkins

---

[Title Page](#)[Abstract](#)[Introduction](#)[Conclusions](#)[References](#)[Tables](#)[Figures](#)[◀](#)[▶](#)[◀](#)[▶](#)[Back](#)[Close](#)[Full Screen / Esc](#)[Print Version](#)[Interactive Discussion](#)

EGU

---

**Convective damping  
of buoyancy  
anomalies**I. Folkins

---

[Title Page](#)[Abstract](#)[Introduction](#)[Conclusions](#)[References](#)[Tables](#)[Figures](#)[◀](#)[▶](#)[◀](#)[▶](#)[Back](#)[Close](#)[Full Screen / Esc](#)[Print Version](#)[Interactive Discussion](#)

EGU

becomes saturated and unable to undergo further evaporative cooling. The existence of downdrafts above the melting level therefore depends on a continual resupply of dry air to convective regions by the large scale circulation (exception to this argument will occur in situations of high condensate loading). The transition from a conditionally stable to unstable atmosphere at the melting level may account for the dramatic increase in downdraft mass flux near this height (May and Rajopadhyaya, 1999).

Updrafts which contain condensate are also subject to self damping due to dry air entrainment. In the atmosphere, the saturated water vapor pressure decreases with height much more rapidly than the density. This means that water vapor phase changes have the potential to have a much greater relative impact on the heat budget of an air parcel in the lower troposphere. One would therefore expect the evaporation or condensation of condensate associated with dry air entrainment to have a bigger impact on reducing the convective damping timescale in the lower troposphere.

## 8. Spatial variability

In general, the climatological total divergence at any given location in the tropics will be non-zero. For example, locations characterized by persistent deep convection will tend to be convergent in the lower troposphere, while locations characterized by a greater prevalence of shallow convection (considered here to be convection which rarely extends beyond the melting level inversion) will tend to be divergent. The total divergence in actively convecting regions, and therefore also the divergence of the background atmosphere, is required to go to zero only when averaged over spatial scales comparable with the Rossby radius. In a sense, this paper has used extensive averaging of many radiosonde profiles ( $\sim 2000$ ) at individual locations as a surrogate for estimating  $\overline{\delta_b}$ . However, it is not clear why a spatially averaged constraint on the total and convective divergences should give rise to what appears to be a local constraint on the climatological radiative mass flux. One explanation is that the temperature profile at a given location, unlike the divergence itself, is a nonlocal reflection of the influence of all grav-

ity waves within a distance of one Rossby deformation radius.

It is also likely that the constraint on  $\delta_b$  only reduces to a local constraint on the radiative mass flux at locations surrounded by homogeneous active deep oceanic convection on a spatial scale larger than one Rossby radius. Figure 8 shows the climatological rainfall pattern in the region of the SPARC Western Equatorial Pacific radiosonde stations. This pattern was obtained by averaging over the  $2.5^\circ$  by  $2.5^\circ$  monthly mean rainfall estimates from the Global Precipitation Climatology Project (GPCP) Version 2 Combined Precipitation Data Set (Huffman et al., 1997) from 1991 to 2000. In addition to showing the locations of the Koror, Yap, and Truk radiosonde stations, Fig. 8 also shows the locations of radiosonde stations at Ponape and Majuro. The annual mean static stability and clear sky radiative mass flux profiles of these two stations are shown in Fig. 9. While the climatological rainfall rate at these two locations is quite high, rainfall is somewhat more strongly spatially localized at Ponape and Majuro than at the other three radiosonde locations. This may explain why the climatological radiative mass flux divergence at Ponape and Majuro is between 2 km and 5.2 km larger than at the other three radiosonde stations.

## 9. Conclusions

One usually thinks of convective adjustment as a process by which convective heat sources impose a density profile on the background atmosphere. This viewpoint is incomplete, however, because the horizontal and vertical motions forced on the background atmosphere by buoyancy anomalies necessarily involve a net entrainment of mass into, or detrainment of mass away, from convective heat sources. These processes can have a significant impact on the densities within updrafts and downdrafts (especially at warmer temperatures), so there is no reason to anticipate a priori that the densities within convective plumes will conform to either the undilute reversible adiabatic or pseudoadiabatic idealizations.

In the middle troposphere (5.2 km–10 km), lapse rates do follow a moist pseudoadi-

## Convective damping of buoyancy anomalies

I. Folkins

Title Page

Abstract

Introduction

Conclusions

References

Tables

Figures

◀

▶

◀

▶

Back

Close

Full Screen / Esc

Print Version

Interactive Discussion

## Convective damping of buoyancy anomalies

I. Folkins

Title Page

Abstract

Introduction

Conclusions

References

Tables

Figures

◀

▶

◀

▶

Back

Close

Full Screen / Esc

Print Version

Interactive Discussion

EGU

abatic profile to a high degree of accuracy. Although the reasons for the validity of the pseudoadiabatic approximation in this region of the atmosphere are unclear, it is likely that the rapid decrease in condensate loading of oceanic updrafts just above the melting level (e.g. Jorgensen et al., 1985) is a contributing factor. Not only would this loss of condensate make ascent in these updrafts more consistent with pseudoadiabatic assumptions, it would also tend to reduce the impact of any dry air entrainment (and its associated evaporative cooling) on the temperature and buoyancy of these updrafts.

In the lower troposphere, where lapse rates deviate significantly from both reversible adiabatic and pseudoadiabatic assumptions, the question arises as to whether there exists any simple constraint on tropical temperatures in this region of the atmosphere. It is possible that no such constraint exists, and that observed temperatures simply reflect the condensate loading, and particular rates of entrainment and detrainment, of updrafts and downdrafts in the lower tropical troposphere. In this case, the rates of these small scale processes would not be prescribed by larger-scale considerations. There would be no fundamental explanation for the observed density structure of the lower troposphere, and the cumulus parameterization problem would be more likely to be insoluble.

The paper has attempted to motivate a new constraint on temperatures in the lower tropical troposphere by considering the way in which divergence anomalies in the tropics interact with themselves, and with other buoyancy anomalies in their surroundings. The total divergence, averaged over some region, can be decomposed into a convective divergence, and a divergence associated with radiative cooling of the background atmosphere:  $\overline{\delta_t} = \overline{\delta_c} + \overline{\delta_b}$ . It was shown, using the ECMWF ERA-40 reanalyses, that the total divergence  $\overline{\delta_t}$  decays to zero on a spatial scale that, as would be expected, is approximately equal to the Rossby radius of deformation of the gravity waves likely to dominate divergence patterns in the lower tropical troposphere. Ordinarily, one would attribute the finite spatial scale of divergence anomalies in the tropical lower troposphere to two types of damping. One type of damping is associated with an induced radiative divergence in the background atmosphere. It is the usual mechanism

---

**Convective damping  
of buoyancy  
anomalies**I. Folkins

---

[Title Page](#)[Abstract](#)[Introduction](#)[Conclusions](#)[References](#)[Tables](#)[Figures](#)[◀](#)[▶](#)[◀](#)[▶](#)[Back](#)[Close](#)[Full Screen / Esc](#)[Print Version](#)[Interactive Discussion](#)

EGU

whereby buoyancy anomalies influence temperatures in the background atmosphere. Divergence anomalies can also be damped by inducing a compensating divergence in neighboring updrafts and downdrafts, and by generating an exchange of mass with the background atmosphere which has a strong negative feedback on their own buoyancy. The relative importance of the radiative and convective damping mechanisms depends on the timescales associated with each process. Measurements of temperature, water vapor concentration, and condensate loading inside both updrafts and downdrafts have consistently demonstrated that buoyancy anomalies in the lower tropical troposphere are extremely weak, at least over the oceans. This would imply that buoyancy anomalies in the lower tropical troposphere are strongly damped. Radiative transfer calculations show that the climatological clear sky radiative divergence in the lower tropical troposphere is near zero. It is therefore likely that the radiative damping timescale in this region of the atmosphere is too long to explain the weakness of observed buoyancy anomalies, and therefore, that the convective damping of buoyancy anomalies is highly efficient in the lower tropical troposphere.

The vertical variation of the density in the lower troposphere is an important unsolved problem in tropical meteorology. No model has yet been able to reproduce the detailed structure of the observed lapse rate shown in Fig. 1. Part of the difficulty is that it may involve coupling processes at very different spatial scales: i.e. gravity wave propagation over distances comparable with the Rossby radius, and the small scale effects of turbulent entrainment and detrainment on the buoyancies of updrafts and downdrafts. Although there has been considerable previous discussion on how the stability anomalies near the freezing level might be related to the melting or freezing of water (e.g. Johnson et al., 1999), this has been the first attempt to quantitatively account for the vertical variation of the lapse rate in the lower troposphere. Clearly, however, a definitive explanation would involve a more predictive, dynamical model than the diagnostic approach adopted here, where we have tried to make inferences from observed densities and heating rates. We have also taken the point of view that the freezing level denotes a change between two different convective regimes, rather than viewing these

anomalies as a localized reflection of heating and/or freezing.

Deep convective systems are typically convergent in the lower troposphere. (Between 2.0–5.2 km, this convergence presumably mainly supplies a downwardly increasing downdraft mass flux). In this paper, it has been argued that the convective divergence is required to go to zero when averaged over spatial scales comparable with the Rossby radius. In this case, it would be necessary for the lower tropospheric convergence of deep convective clouds to be balanced, on the regional scale, by a divergence from shallow convection. The resulting coupling between deep and shallow convection may be of relevance to the propagation of some tropical convective disturbances, such as the Madden Julian Oscillation (MJO). As it propagates toward the east, the large scale envelope of deep convection associated with an MJO event is preceded by a zone of shallow convection, which by moistening the lower troposphere up to the melting level (Kemball-Cook and Weare, 2001; Kikuchi and Takayabu, 2004), presumably preconditions the atmosphere for the subsequent deep convection. It may be possible to interpret the low-level divergence of the shallow convection advancing in front of the MJO, in terms of a constraint on the convective divergence, as a response to the low-level convergence of the deep convection within the MJO.

*Acknowledgements.* ECMWF ERA-40 data used in this study have been provided by ECMWF and obtained from the ECMWF data server. This research was supported by the Natural Sciences and Engineering Research Council of Canada (NSERC), and the Canadian Foundation for Climate and Atmospheric Sciences (CFCAS). This paper has benefited from comments by R. Martin and G. Lesins.

## References

- Bergman, J. W. and Hendon, H. H.: Calculating monthly radiative fluxes and heating rates from monthly cloud distributions, *J. Atmos. Sci.*, 55, 3471–3491, 1998.
- 25 Betts, A. K.: Saturation point analysis of moist convective overturning, *J. Atmos. Sci.*, 39, 1484–1505, 1982.

---

## Convective damping of buoyancy anomalies

I. Folkins

---

Title Page

Abstract

Introduction

Conclusions

References

Tables

Figures

◀

▶

◀

▶

Back

Close

Full Screen / Esc

Print Version

Interactive Discussion

---

**Convective damping  
of buoyancy  
anomalies**

---

I. Folkins

---

[Title Page](#)[Abstract](#)[Introduction](#)[Conclusions](#)[References](#)[Tables](#)[Figures](#)[◀](#)[▶](#)[◀](#)[▶](#)[Back](#)[Close](#)[Full Screen / Esc](#)[Print Version](#)[Interactive Discussion](#)

EGU

- Bolton, D.: The computation of equivalent potential temperature, *Mon. Wea. Rev.*, 108, 1046–1053, 1980.
- Bretherton, C. S. and Smolarkiewicz, P. K.: Gravity waves, compensating subsidence and detrainment around cumulus clouds, *J. Atmos. Sci.*, 46, 740–759, 1989.
- 5 Doherty, G. M. and Newell, R. E.: Radiative effects of changing atmospheric water vapour, *Tellus*, 36 B, 149–162, 1984.
- Emanuel, K. A. and Bister, M.: Moist convective velocity and buoyancy scales, *J. Atmos. Sci.*, 53, 3276–3285, 1996.
- Folkens, I. and Martin, R. V.: The vertical structure of tropical convection, and its impact on the  
10 budgets of water vapor and ozone, *J. Atmos. Sci.*, 62, 1560–1573, 2005.
- Fu, Q. and Liou, K. N.: On the correlated k-distribution method for radiative transfer in nonhomogeneous atmospheres, *J. Atmos. Sci.*, 49, 2139–2156, 1992.
- Gettelman, A., Forster, P. M., Fujiwara, M., et al.: Radiation balance of the tropical tropopause layer, *J. Geophys. Res.*, 109, D07103, doi:10.1029/2003JD004190, 2004.
- 15 Holton, J. R.: *An Introduction to Dynamic Meteorology*, Academic, New York, 1992.
- Huffman, G. J., Adler, R. F., Arkin, P. A., et al.: The Global Precipitation Climatology Project (GPCP) Combined Precipitation Data Set, *Bull. Amer. Meteor. Soc.*, 78, 5–20, 1997.
- Johnson, R. H., Rickenbach, T. M., Rutledge, S. A., et al.: Trimodal characteristics of tropical convection, *J. Atmos. Sci.*, 12, 2397–2418, 1999.
- 20 Jorgensen, D. P., Zipser, E. J., and LeMone, M. A.: Vertical motions in hurricanes, *J. Atmos. Sci.*, 42, 839–856, 1985.
- Jorgensen, D. P. and LeMone, M. A.: Vertical velocity characteristics of oceanic convection, *J. Atmos. Sci.*, 46, 621–640, 1989.
- Kemball-Cook, S. R. and Weare, B. C.: The onset of convection in the Madden-Julian Oscillation, *J. Atmos. Sci.*, 14, 780–793, 2001.
- 25 Kikuchi, K. and Takayabu, Y. N.: The development of organized convection associated with the MJO during TOGA COARE IOP: Trimodal characteristics, *Geophys. Res. Lett.*, 31, L10101, doi:10.10292004GL019601, 2004.
- Lucas, C., Zipser, E. J., and LeMone, M. A.: Vertical velocity in oceanic convection off tropical Australia, *J. Atmos. Sci.*, 51, 3183–3193, 1994.
- 30 Mapes, B. E. and Houze, R. A.: Diabatic divergence profiles in Western Pacific mesoscale convective systems, *J. Atmos. Sci.*, 52, 1807–1828, 1995.
- Mapes, B. E. and Zuidema, P.: Radiative-dynamical consequences of dry tongues in the tropical

- troposphere, *J. Atmos. Sci.*, 53, 620–638, 1996.
- Mapes, B. E.: Water's two scale heights: The moist adiabat and the radiative troposphere, *Q. J. R. Meteor. Soc.*, 127, 2353–2366, 2001.
- 5 May, P. T. and Rajopadhyaya, D. K.: Vertical velocity characteristics of deep convection over Darwin, Australia, *Mon. Wea. Rev.*, 127, 1056–1071, 1999.
- Newman, M., Sardeshmukh, P. D., and Bergman, J. W.: An assessment of the NCEP, NASA, and ECMWF reanalyses over the Tropical West Pacific warm pool, *Bull. Amer. Meteor. Soc.*, 81, 41–48, 2000.
- 10 Rodgers, C. D. and Walshaw, C. D.: The computation of infra-red cooling rate in planetary atmospheres, *Quart. J. Roy. Meteor. Soc.*, 92, 67–92, 1966.
- Wei, D., Blyth, A. M., and Raymond, D. J.: Buoyancy of convective clouds in TOGA COARE, *J. Atmos. Sci.*, 55, 3381–3391, 1998.
- Xu, K. and Emanuel, K. A.: Is the tropical atmosphere conditionally unstable?, *J. Atmos. Sci.*, 117, 1471–1479, 1989.

---

**Convective damping  
of buoyancy  
anomalies**I. Folkins

---

[Title Page](#)[Abstract](#)[Introduction](#)[Conclusions](#)[References](#)[Tables](#)[Figures](#)[I◀](#)[▶I](#)[◀](#)[▶](#)[Back](#)[Close](#)[Full Screen / Esc](#)[Print Version](#)[Interactive Discussion](#)

## Convective damping of buoyancy anomalies

I. Folkins

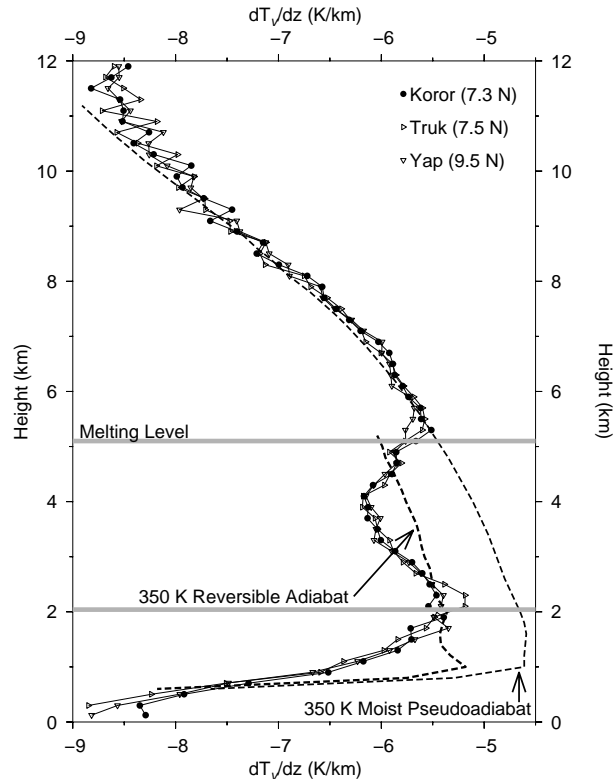


**Fig. 1.** Annual mean profiles of  $dT_v/dz$  at 3 radiosonde locations within the Western Tropical Pacific Warm Pool. The profiles were generated from radiosonde measurements, taken up to twice daily, from 1999–2001. The dashed line is the  $dT_v/dz$  of a pseudoadiabat starting from the surface with a relative humidity of 80% and  $\theta_{ep}=350$  K. The dotted line is the  $dT_\rho/dz$  of a reversible moist adiabat starting from the surface with a relative humidity of 80% and  $\theta_e=350$  K. The radiosonde data was downloaded from the SPARC (Stratospheric Processes and their Role in Climate) Data Center (<http://www.sparc.sunysb.edu>).

Title Page

Abstract

Introduction

Conclusions

References

Tables

Figures

◀

▶

◀

▶

Back

Close

Full Screen / Esc

Print Version

Interactive Discussion

## Convective damping of buoyancy anomalies

I. Folkins

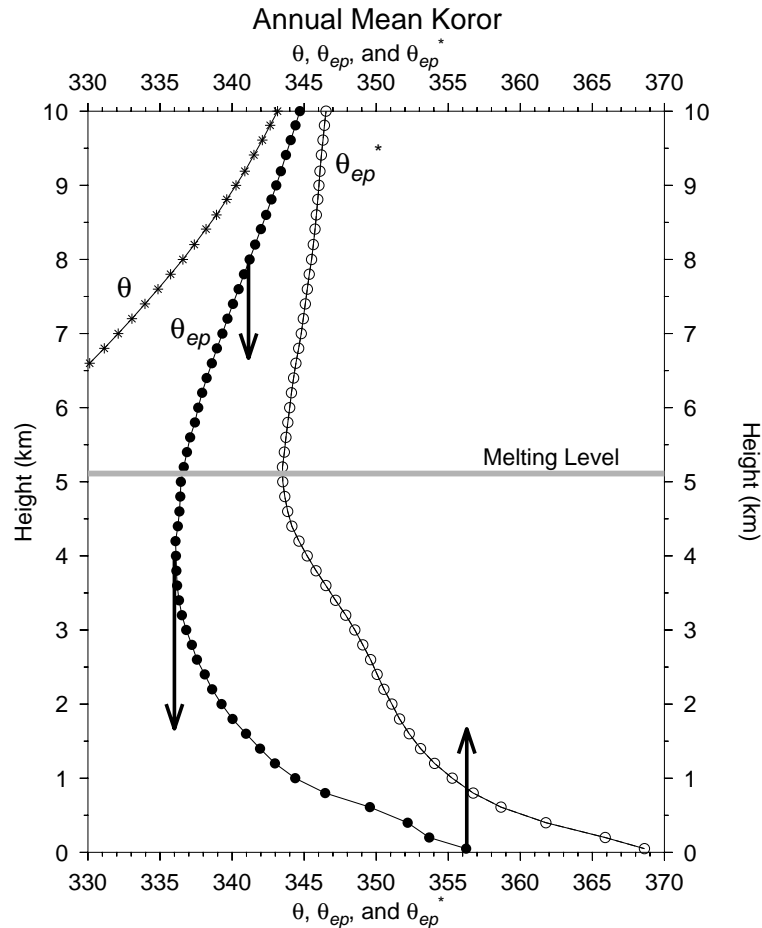


**Fig. 2.** The curves represent the annual mean potential temperature ( $\theta$ , asterisks), pseudoequivalent potential Temperature ( $\theta_{ep}$ , solid circles), and saturated pseudoequivalent potential temperature ( $\theta_{ep}^*$ , squares) profiles at Koror. Note that the melting level occurs near the minimum in  $\theta_{ep}^*$ .

7333

Title Page

Abstract

Introduction

Conclusions

References

Tables

Figures

◀

▶

◀

▶

Back

Close

Full Screen / Esc

Print Version

Interactive Discussion

EGU

**Convective damping  
of buoyancy  
anomalies**

I. Folkins

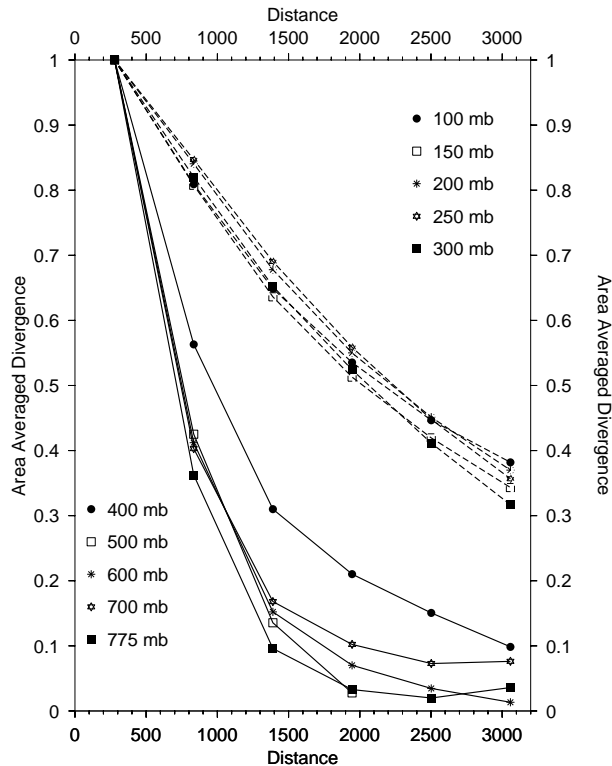


**Fig. 3.** This plot shows how the ECMWF monthly mean divergence from April 2000 responds to the spatial scale over which it is being averaged. It was calculated by starting at grid cells between  $10^{\circ}$  S and  $10^{\circ}$  N with positive divergence, and averaging over progressively larger boxes, centered at the original grid cell, of  $3 \times 3$ ,  $5 \times 5$ ,  $7 \times 7$ ,  $9 \times 9$ , and  $11 \times 11$  grid cells. The divergence profiles generated from each positive divergence anomaly were normalized so that each profile had equal weight, and then averaged together. The spatial scale of a divergence anomaly tends to increase rapidly in going from 400 mb to 300 mb.

[Title Page](#)[Abstract](#)[Introduction](#)[Conclusions](#)[References](#)[Tables](#)[Figures](#)[◀](#)[▶](#)[◀](#)[▶](#)[Back](#)[Close](#)[Full Screen / Esc](#)[Print Version](#)[Interactive Discussion](#)

EGU

## Convective damping of buoyancy anomalies

I. Folkins

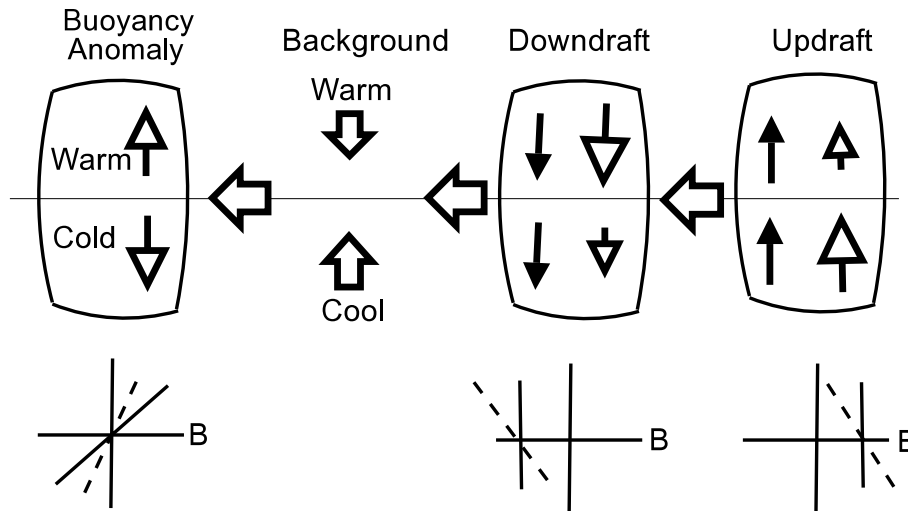


**Fig. 4.** A buoyancy anomaly (warm/cold dipole) is introduced into an atmosphere where there is a downdraft of constant negative buoyancy and mass flux, and an updraft of constant positive buoyancy and mass flux. Solid arrows indicate mass fluxes prior to the introduction of the buoyancy anomaly, while open arrows indicate mass fluxes after the introduction of the buoyancy anomaly. The size of the arrow gives an approximate indication of the magnitude of the mass flux. The plots along the bottom indicate how buoyancy varies with height inside the buoyancy anomaly and inside the updraft/downdraft. Solid lines refer to buoyancies before the atmosphere responds to the buoyancy anomaly, while dashed lines refer to buoyancies after the atmosphere has responded to the buoyancy anomaly. Initially, the vertical mass flux within the buoyancy anomaly is zero. The positive buoyancy gradient within the anomaly induces vertical motions in the background atmosphere which drive a convergent flow toward the anomaly. The temperature changes in the background atmosphere associated with these background vertical velocities give rise to buoyancy gradients, and divergent outflows, from surrounding updrafts and downdrafts.

Title Page

Abstract

Introduction

Conclusions

References

Tables

Figures

◀

▶

◀

▶

Back

Close

Full Screen / Esc

Print Version

Interactive Discussion

EGU

## Convective damping of buoyancy anomalies

I. Folkins

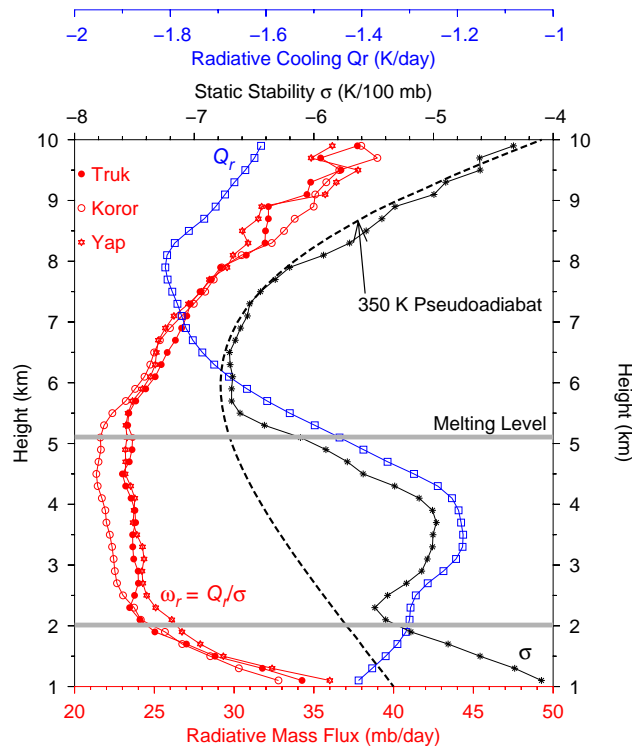


**Fig. 5.** The black line with asterisks shows the annual mean static stability  $\sigma$  at Truk. The dashed line is the static stability of a  $\theta_{ep}=350$  K moist pseudoadiabat. The blue line is the annual mean clear sky radiative heating rate  $Q_r$  calculated from seasonal mean temperature and water vapor profiles at Truk, and tropical mean ozone profiles. It was calculated using a four stream, correlated- $k$  distribution, radiative transfer code (Fu and Liou, 1992). The three red lines refer to the clear sky radiative mass flux  $\omega_r = Q_r/\sigma$  at Truk, Koror, and Yap, calculated from the annual mean  $\sigma$  and  $Q_r$  profiles at each station.

Title Page

Abstract

Introduction

Conclusions

References

Tables

Figures

◀

▶

◀

▶

Back

Close

Full Screen / Esc

Print Version

Interactive Discussion

EGU

## Convective damping of buoyancy anomalies

I. Folkins

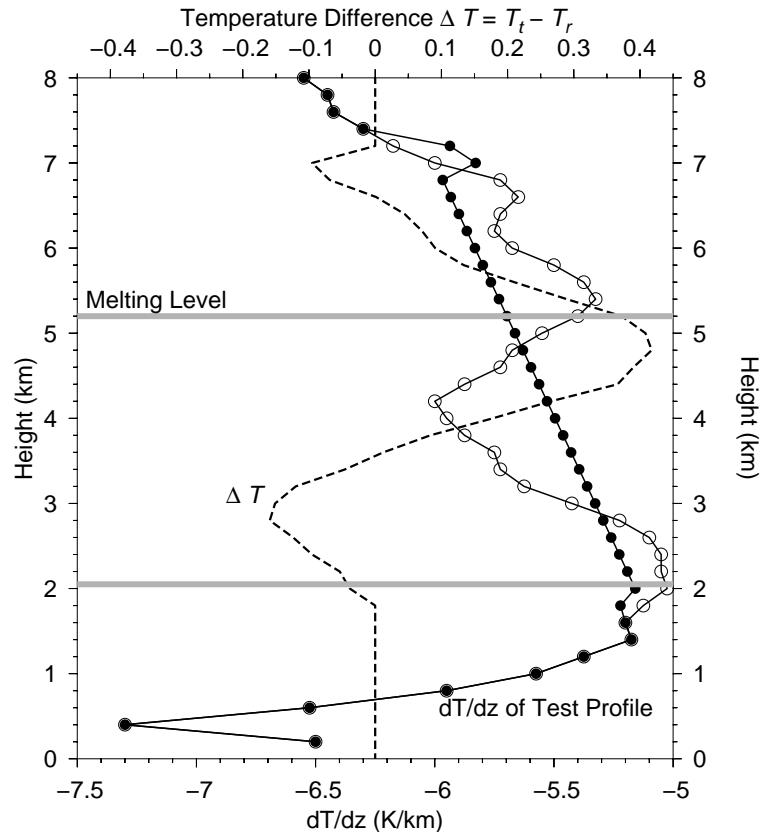


**Fig. 6.** The curve with open circles is the  $dT/dz$  of a reference September–November temperature profile at Koror. The curve with solid circles is the  $dT/dz$  of a test temperature profile in which the temperature is kept unchanged below 1.8 km and above 7.2 km, but interpolated between these two heights in such a way as to give rise to a lapse rate that varies linearly with altitude. The dashed line shows the difference between the test ( $T_t$ ) and reference ( $T_r$ ) temperature profiles.

[Title Page](#)
[Abstract](#)
[Introduction](#)
[Conclusions](#)
[References](#)
[Tables](#)
[Figures](#)
[◀](#)
[▶](#)
[◀](#)
[▶](#)
[Back](#)
[Close](#)
[Full Screen / Esc](#)
[Print Version](#)
[Interactive Discussion](#)

**Convective damping of buoyancy anomalies**

I. Folkins

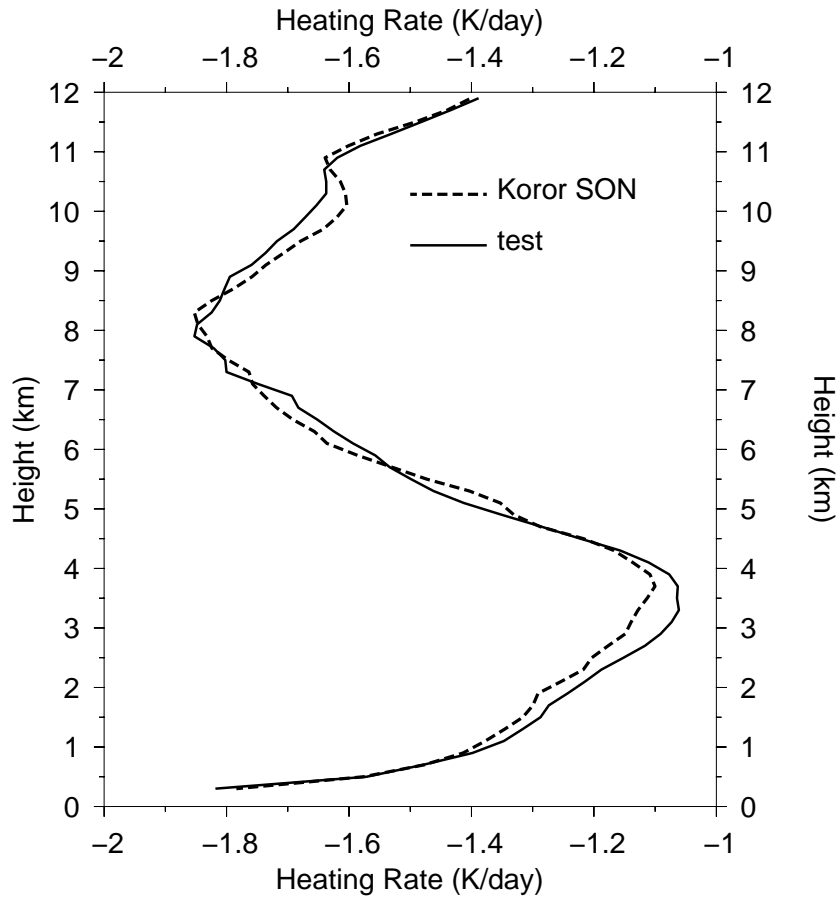


**Fig. 7.** The solid curve shows the clear sky radiative heating rate of the mean September–November temperature profile at Koror. The dashed curve is the radiative heating rate for the temperature profile, adjusted as indicated in Fig. 6.

[Title Page](#)[Abstract](#)[Introduction](#)[Conclusions](#)[References](#)[Tables](#)[Figures](#)[◀](#)[▶](#)[◀](#)[▶](#)[Back](#)[Close](#)[Full Screen / Esc](#)[Print Version](#)[Interactive Discussion](#)

**Convective damping  
of buoyancy  
anomalies**

I. Folkins

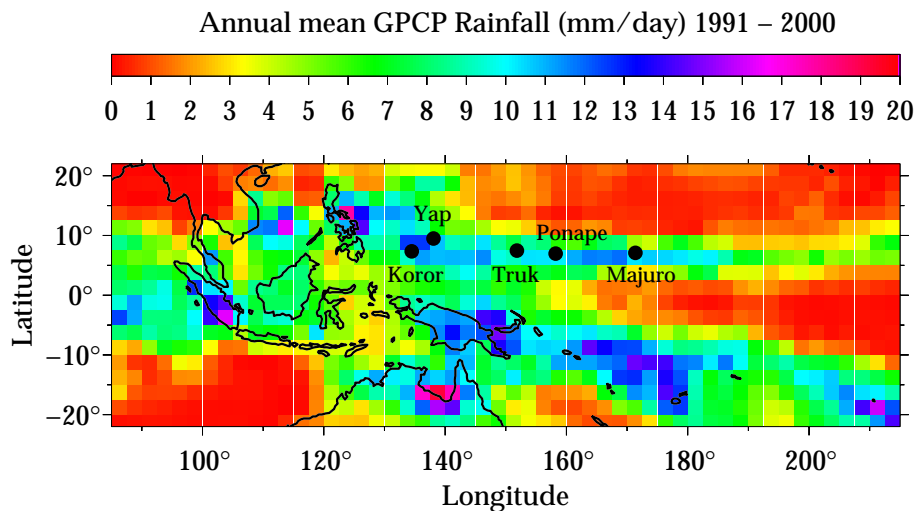


**Fig. 8.** The locations of the five high resolution radiosonde stations discussed in this paper, superimposed on a map of climatological rainfall.

[Title Page](#)[Abstract](#)[Introduction](#)[Conclusions](#)[References](#)[Tables](#)[Figures](#)[◀](#)[▶](#)[◀](#)[▶](#)[Back](#)[Close](#)[Full Screen / Esc](#)[Print Version](#)[Interactive Discussion](#)

EGU

Convective damping of buoyancy anomalies

I. Folkins

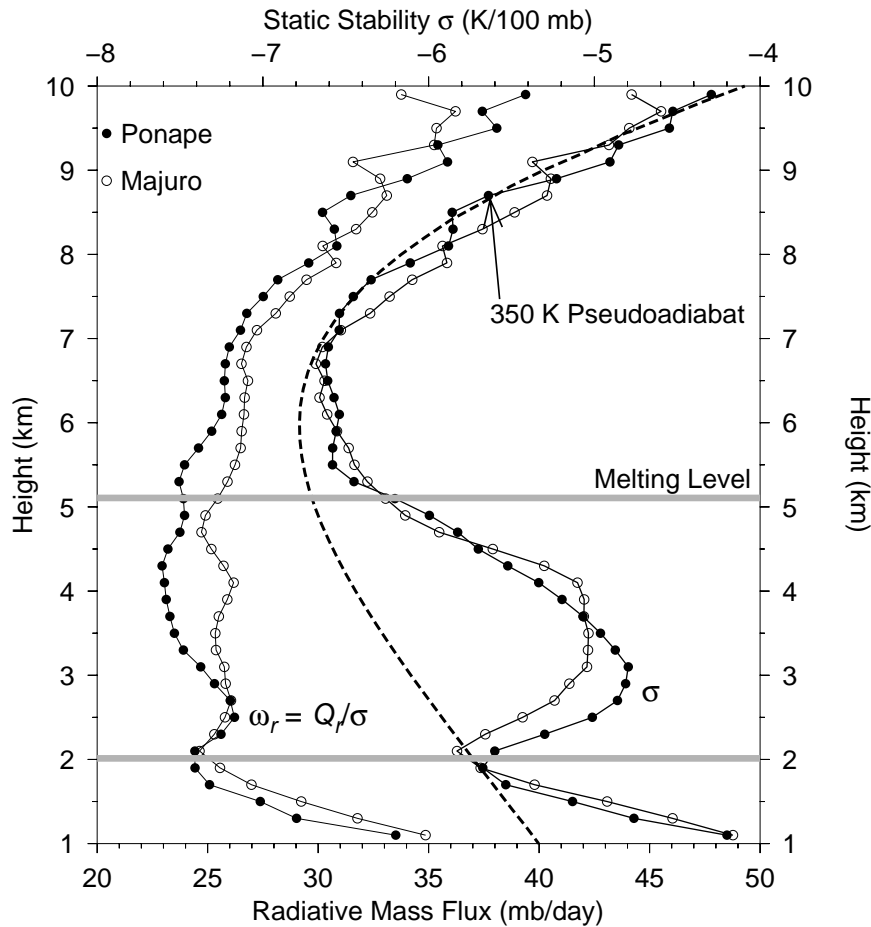


**Fig. 9.** Annual mean static stability ( $\sigma$ ) and clear sky radiative mass flux ( $\omega_r$ ) profiles at Ponape and Majuro. The dashed line is the stability profile of a 350 K moist pseudoadiabat.

Title Page

Abstract

Introduction

Conclusions

References

Tables

Figures

◀

▶

◀

▶

Back

Close

Full Screen / Esc

Print Version

Interactive Discussion